Cement and Concrete Research 40 (2010) 157–166

Contents lists available at ScienceDirect

Cement and Concrete Research

journal homepage: http://ees.elsevier.com/CEMCON/default.asp

Use of bacteria to repair cracks in concrete

Kim Van Tittelboom [a], Nele De Belie [a,*], Willem De Muynck [a,b], Willy Verstraete [b]

[a] Magnel Laboratory for Concrete Research, Ghent University, Department of Structural Engineering, Technologiepark Zwijnaarde 904, B-9052 Ghent, Belgium
[b] Laboratory of Microbial Ecology and Technology (LabMET), Ghent University, Coupure Links 653, B-9000 Ghent, Belgium

ARTICLE INFO

Article history:
Received 18 March 2009
Accepted 27 August 2009

Keywords:
Concrete (E)
Microcracking (B)
$CaCO_3$ (D)
Bacteria

ABSTRACT

As synthetic polymers, currently used for concrete repair, may be harmful to the environment, the use of a biological repair technique is investigated in this study. Ureolytic bacteria such as *Bacillus sphaericus* are able to precipitate $CaCO_3$ in their micro-environment by conversion of urea into ammonium and carbonate. The bacterial degradation of urea locally increases the pH and promotes the microbial deposition of carbonate as calcium carbonate in a calcium rich environment. These precipitated crystals can thus fill the cracks. The crack healing potential of bacteria and traditional repair techniques are compared in this research by means of water permeability tests, ultrasound transmission measurements and visual examination. Thermogravimetric analysis showed that bacteria were able to precipitate $CaCO_3$ crystals inside the cracks. It was seen that pure bacteria cultures were not able to bridge the cracks. However, when bacteria were protected in silica gel, cracks were filled completely.

1. Introduction

In concrete, cracking is a common phenomenon due to the relatively low tensile strength. High tensile stresses can result from external loads, imposed deformations (due to temperature gradients, confined shrinkage, and differential settlement), plastic shrinkage, plastic settlement, and expansive reactions (e.g. due to reinforcement corrosion, alkali silica reaction, sulphate attack). Without immediate and proper treatment, cracks tend to expand further and eventually require costly repair. Durability of concrete is also impaired by these cracks, since they provide an easy path for the transport of liquids and gasses that potentially contain harmful substances. If micro-cracks grow and reach the reinforcement, not only the concrete itself may be attacked, but also the reinforcement will be corroded when it is exposed to water and oxygen, and possibly carbon dioxide and chlorides. Micro-cracks are therefore precursors to structural failure [1].

For crack repair, a variety of techniques is available but traditional repair systems have a number of disadvantageous aspects such as different thermal expansion coefficient compared to concrete and environmental and health hazards. Therefore, bacterially induced calcium carbonate precipitation has been proposed as an alternative and environmental friendly crack repair technique. In 1995, Gollapudi et al. ([2] as quoted by [3]), were the first to introduce this novel technique in fixing cracks with environmentally friendly biological processes.

The microbial precipitation of $CaCO_3$ is determined by several factors including: the concentration of dissolved inorganic carbon, the pH, the concentration of calcium ions and the presence of nucleation sites. The first three factors are provided by the metabolism of the bacteria while the cell wall of the bacteria will act as a nucleation site [4].

The bacteria used in this research produce urease which catalyzes the hydrolysis of urea ($CO(NH_2)_2$) into ammonium (NH_4^+) and carbonate (CO_3^{2-}). First, 1 mol of urea is hydrolysed intracellular to 1 mol of carbamate and 1 mol of ammonia (Eq. (1)). Carbamate spontaneously hydrolyses to form additionally 1 mol of ammonia and carbonic acid (Eq. (2)). These products subsequently form 1 mol of bicarbonate and 2 mol of ammonium and hydroxide ions (Eqs. (3) and (4)). The last 2 reactions give rise to a pH increase, which in turn shifts the bicarbonate equilibrium, resulting in the formation of carbonate ions (Eq. (5)) [5].

$$CO(NH_2)_2 + H_2O \rightarrow NH_2COOH + NH_3 \quad (1)$$

$$NH_2COOH + H_2O \rightarrow NH_3 + H_2CO_3 \quad (2)$$

$$H_2CO_3 \leftrightarrow HCO_3^- + H^+ \quad (3)$$

$$2NH_3 + 2H_2O \leftrightarrow 2NH_4^+ + 2OH^- \quad (4)$$

$$HCO_3^- + H^+ + 2NH_4^+ + 2OH^- \leftrightarrow CO_3^{2-} + 2NH_4^+ + 2H_2O \quad (5)$$

Since the cell wall of the bacteria is negatively charged, the bacteria draw cations from the environment, including Ca^{2+}, to deposit on their cell surface. The Ca^{2+}-ions subsequently react with

* Corresponding author. Tel.: +32 9 264 55 22; fax: +32 9 264 58 45.
E-mail address: nele.debelie@ugent.be (N. De Belie).

0008-8846/$ – see front matter © 2009 Elsevier Ltd. All rights reserved.
doi:10.1016/j.cemconres.2009.08.025

the CO_3^{2-}-ions, leading to the precipitation of $CaCO_3$ at the cell surface that serves as a nucleation site (Eqs. (6) and (7)).

$$Ca^{2+} + \text{Cell} \rightarrow \text{Cell-}Ca^{2+} \quad (6)$$

$$\text{Cell-}Ca^{2+} + CO_3^{2-} \rightarrow \text{Cell-}CaCO_3\downarrow \quad (7)$$

Several bacteria have the ability to precipitate calcium carbonate. These bacteria can be found in soil, sand, natural minerals,... [6]. In their study, Jonkers et al. [6,7] used *Bacillus cohnii* bacteria to precipitate $CaCO_3$. *Bacillus pasteurii* have been used by Santhosh et al. [8], Day et al. [9], Bang et al. [10] and Ramakrishnan et al. [11], while Dick et al. [5] used *Bacillus lentus* and *Bacillus sphaericus*. In this study *B. sphaericus* bacteria will be used to heal cracks in concrete. Selection of this spore forming strain was based upon earlier work [5]. This strain showed a high urease activity, a continuous formation of dense calcium carbonate crystals and a very negative zeta-potential.

In the aforementioned studies, calcium carbonate precipitation has been used for consolidation of sand columns, healing of cracks in granite or for surface treatment of limestone. For these applications the use of bacteria, precipitating $CaCO_3$, proved its efficiency. However, when bacteria are used to heal cracks in concrete, the major hindering factor is the highly alkaline pH of concrete, restricting the growth of the bacteria. Therefore, it is necessary to immobilize the bacterial cells and to protect them from the high pH in concrete. Polyurethane (PU) has been widely used as a vehicle for immobilization of enzymes and whole cells because of its mechanical strength and biochemical inertness [9–12]. Bang et al. [10] used cylindrical-shaped PU-foam, containing bacterial cells, with an average dimension of 10 mm (diameter) × 50 mm (length). The prepared PU-foam strip was placed into simulated cracks and in this way used as crack repair technique. Since this treatment is time-consuming and only suitable for wide cracks (Bang et al. used cracks with a width of 3.18 mm [10]), silica gel was used in this study to immobilize the bacteria [13]. The gel, containing the bacteria, can be directly sprayed into the crack with a syringe. The silica gel was not only used to immobilize the bacteria but it was also used as filling material to fill the cracks before $CaCO_3$ precipitation started.

A lot of research on bacterial $CaCO_3$ precipitation has been conducted with calcium chloride ($CaCl_2.2H_2O$) as calcium source [14]. Since chloride ions may be detrimental for the concrete reinforcement, the use of calcium nitrate ($Ca(NO_3)_2.4H_2O$) and calcium acetate ($Ca(CH_3COO)_2.H_2O$), as alternative calcium sources, was investigated in this study.

The efficiency of the microbially induced $CaCO_3$ precipitation to heal cracks in concrete was defined by performing low pressure water permeability tests, ultrasonic measurements and also by visual examination of the degree of crack filling. A comparison was made between the microbial repair technique and traditional methods used to repair cracks in concrete, more particularly epoxy and grout injection. Furthermore, a comparison was made between biological treatments with active or autoclaved bacteria, through performance of a thermogravimetric analysis.

2. Materials and methods

2.1. Concrete samples

Concrete samples were made by using ordinary Portland cement CEM I 52.5 N. The composition of the concrete mix is shown in Table 1. Moulds with dimensions of 150 mm × 150 mm × 150 mm, 150 mm × 150 mm × 600 mm and 160 mm × 160 mm × 70 mm were used. After casting, all moulds were placed in an air-conditioned room with a temperature of 20 °C and a relative humidity of more than 90% for a period of 24 h. After demoulding, the specimens were placed in the same air-conditioned room for at least 27 days. Concrete samples used for the water permeability test were cured for more than one year to assure more complete hydration (see further). 28 days after preparation of the concrete, compression strength was determined on the concrete cubes (150 mm × 150 mm × 150 mm). The mean compression strength was 55.2 N/mm^2 with a standard deviation of 2.19 N/mm^2.

Table 1
Composition of concrete mix.

Material	Volume [kg/m³]
Sand 0/4	670
Aggregates 2/8	490
Aggregates 8/16	790
CEM I 52.5 N	300
Water	150

2.2. Creation of cracks

Cracked concrete samples were prepared in two different ways. The first method resulted in samples with standardized cracks while the second method gave rise to more realistic cracked samples.

2.2.1. Standardized cracks

Standardized cracks were realized in concrete samples with dimensions of 160 mm × 160 mm × 70 mm. A thin copper plate of 0.3 mm thickness was introduced in the fresh concrete paste up to a depth of 10 mm or 20 mm. The moulds with the copper plates are shown in Fig. 1. The plates were removed during demoulding, after 24 h, resulting in prisms with a narrow groove on the upper surface, with a depth of 10 mm or 20 mm and a width of 0.3 mm.

2.2.2. Realistic cracks

More realistic cracks were obtained by performing splitting tests on concrete cylinders wrapped in fiber reinforced polymer (FRP). From concrete prisms (150 mm × 150 mm × 600 mm), cylinders of 80 mm diameter were taken. From each cylinder of 150 mm height two cylinders of 75 mm height were obtained. These cylinders were covered with tape, and afterwards glass fiber reinforcement (Syncotape 625 g/m^2) was glued around the cylinders by means of an epoxy resin (2-component epoxy PC 5800). The tape served to avoid contact between the epoxy resin and the concrete samples so that after removal of the glass fiber reinforcement intact samples were obtained. After the epoxy had hardened, the cylinders were subjected to a splitting test, as shown in Fig. 2. An Amsler 100 D66/45 testing

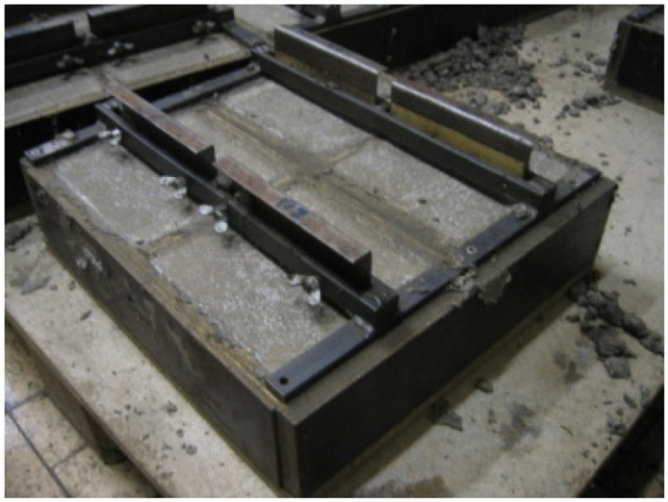

Fig. 1. Creation of standardized cracks.

machine was used to perform the splitting tests. Samples were loaded until a crack was visible with the naked eye. After splitting, each 75 mm high specimen, was sawn into three pieces of 20 mm height. After removal of the glass fiber reinforcement and the tape, samples were again protected with tape at the upper and lower surface and at the side surface near the crack opening. Then, the samples were glued into a PVC ring by the use of epoxy resin (2-component epoxy PC 5800). The PVC ring had an outer diameter of ± 109 mm and an inner diameter of ± 93 mm, the height was 30 mm. The tape prevented the epoxy to come into contact with the upper and lower side of the cylindrical specimen or to flow into the crack. After hardening of the epoxy, the tape was removed.

When the samples were glued in PVC rings, the crack width of each sample was measured by using the computer software ImageJ [15]. First, each sample was scanned, together with a piece of millimetre paper, by means of a color image scanner (CanoScan 3000F). Next, the images were analyzed. By counting the pixel width of the crack and comparing this with the amount of pixels occupied by 1 cm of the millimetre paper, the width of the crack could be determined. Crack width was measured in this way at 15 different locations, equally divided along the crack length. From these measurements, the average width was calculated and this value was used to characterize the crack width of each specimen. Cracked samples with mean crack widths ranging from 0.05 mm to 0.87 mm were obtained. The standard deviation always remained smaller than 0.043 mm.

2.3. Crack repair techniques

2.3.1. Traditional

In this research, two traditional repair techniques were used for comparison with the bacterial $CaCO_3$ precipitation technique. Cracks were repaired by the use of a 2-component epoxy resin (Sikadur 52) and a 2-component cement-bound mortar (SikaTop 111). Before treatment, the samples were made dust-free and dry by the use of a soft brush. Near the crack, at a distance of about 0.5 cm, a tape was applied, so only a small zone around the crack would be influenced by the repair material. The epoxy resin and the mortar were prepared according to the indications supplied with the products. The 2-component epoxy resin was injected in the crack by the use of an injection needle. The cement-bound mortar (grout) was applied using a spatula. The samples with realistic cracks, obtained from the splitting test, were treated on both sides. Samples with standardized cracks were only treated at the side containing the crack.

2.3.2. Bacteria

Cracks were also repaired by the use of $CaCO_3$ precipitating bacteria. Within the framework of previous research, *B. sphaericus* (BS) strains had been isolated from calcareous sludge coming from a biocatalytic ureolytic calcification reactor. On the basis of their morphology six unique strains were distinguished. The purified strains had been deposited at the BCCM culture collection in Ghent, with the serial numbers LMG 222 55 till LMG 222 60. For this purpose, the strain LMG 222 57 was chosen for the treatment of the samples because of its optimal $CaCO_3$ precipitation capabilities [5]. To protect the bacteria from the strong alkaline environment in concrete, the bacteria were, for some of the treatments, immobilized in silica gel. In this research, Levasil®200/30% sol, with a specific surface area of 200 m^2/g and a solids content of 30%, has been used. After treatment of the cracks, as described below, samples were placed in an equimolar urea–calcium solution. Samples were removed from the solution after 3 days, and left to dry for 3 days at 28 °C. Since the cracked samples, obtained from the splitting test, have a continuous crack, they were treated on both sides and they were completely immersed in the solution. The concrete prisms with the standardized cracks show only a crack at one side, so these samples were placed in the solution on plastic rods in such a manner that the liquid level raised 20 mm above the cracked and treated side of the specimens. Different bacterial treatments were carried out, as described below.

Fig. 2. Creation of realistic cracks.

2.3.2.1. BS in sol–gel + $CaCl_2$ or BS in sol–gel + $Ca(NO_3)_2$ or BS in sol–gel + $Ca(CH_3COO)_2$. First, 1.2 g NaCl was added to 10 ml demineralized water and the mixture was vortexed during 30 seconds. Then, 50 ml of an overnight grown culture was centrifuged during 5 minutes at 4 °C and 7000 rpm. The resulting pellet was suspended in the NaCl solution and vortexed during 30 seconds. Afterwards, 40 ml Levasil sol was added and the whole was vortexed again. The obtained suspension was brought into the crack by means of a syringe. When gel-formation began, this treatment was repeated until the entire crack was filled. After hardening of the sol into a gel, the samples were immersed during 3 days in an equimolar solution of urea (20 g/L) and $CaCl_2.2H_2O$ (49 g/L) or $Ca(NO_3)_2.4H_2O$ (79 g/L) or $Ca(CH_3COO)_2.H_2O$ (59 g/L).

2.3.2.2. Sol–gel. Again 1.2 g NaCl was added to 10 ml demineralized water and vortexed during 30 seconds. Then, 40 ml Levasil sol was added and the solution was vortexed again. By means of a syringe, the obtained suspension was brought into the crack and this was repeated until the entire crack was filled.

2.3.2.3. BS + $CaCl_2$. The samples were immersed for 24 h in a *B. sphaericus* culture grown overnight. The growth medium consisted of 20 g/L yeast extract and 20 g/L urea. After this inoculation, specimens were wiped with a paper towel to remove some bacteria from the surface so ureolytic activity primarily resulted from bacteria inside the cracks. Afterwards, samples were immersed for 3 days in an equimolar solution of urea (20 g/L) and $CaCl_2.2H_2O$ (49 g/L).

2.3.2.4. Sol–gel + BS + $CaCl_2$. First, samples were treated with sol–gel as described above. After several days, when the sol–gel was hardened, samples were subjected to the BS + $CaCl_2$ treatment.

2.3.2.5. Autoclaved BS in sol–gel + $CaCl_2$ or autoclaved BS in sol–gel + $Ca(CH_3COO)_2$. For the water permeability test, samples were not only treated with active bacteria, but also with autoclaved bacteria. This was done in order to be sure that the decrease in water flow was not only due to crack filling by silica sol–gel and biomass. The treatment with autoclaved bacteria is analogous to the first biological treatment described above, except that the bacteria culture was autoclaved before centrifugation.

In Table 2, an overview of all the techniques that were used to repair the concrete cracks is given.

2.4. Evaluation of crack repair

2.4.1. Water permeability

The efficiency of the different crack repair techniques was investigated by measuring the water permeability of the cracked

concrete specimens. The used test method is a slightly modified version of the low pressure water permeability test described by Wang et al. [16] and Aldea et al. [17]. By generating water pressure at the top of the samples, by means of a water column, and by following the descent of the water column in time, the water permeability coefficient could be determined.

Test specimens with realistic cracks, obtained from the splitting test, were used for this experiment. For each crack repair technique, 3–4 samples, with their crack widths equally divided in the range from 0.01 mm to 0.9 mm, were treated. When all cracks were treated, samples were vacuum saturated in demineralized water as described by NBN B 24–213 [18]. Vacuum state was held in the vacuum chamber during 2 1/2 h. Afterwards, while maintaining the vacuum situation, demineralized water was added. When samples were completely submerged the atmospheric pressure was restored. After samples remained submerged during 24 h, they were ready for the water permeability test.

The test specimens, glued in PVC rings, were mounted between two cylindrical compartments made of plexiglass as shown in Fig. 3. Rubber seals between the plexiglass and PVC rings were used to ensure a water-tight setup. At the outer end of the plexiglass rings, square cover plates, with 2 holes each, were applied and the cell was clamped together with four threaded bars. In one opening in the upper plate a glass pipette with an inner diameter of 10 mm was positioned and it was covered to avoid evaporation. A piece of millimetre paper was adhered to the pipette for measuring the descent of the water column. In the lower plate hole a rubber drain tube was attached and the free end of this tube was positioned level with the lower end of the concrete sample. The two other holes in the top and bottom plate were sealed with a plug and served to fill both upper and lower cell, including pipette and drain tube, with de-demineralized water.

The drop in water level in the pipette, due to water flow through the cracked specimen, was measured at regular time intervals, normally once a day, depending on the water flow rate of the specimen, and water was restored each time to the original level. Darcy's law (Eq. (8)) was used to calculate the coefficient of water permeability k.

$$k = \frac{aT}{At}\ln\left(\frac{h_0}{h_f}\right) \tag{8}$$

where

a cross-sectional area of pipette [m^2]
A cross-sectional area of specimen [m^2]

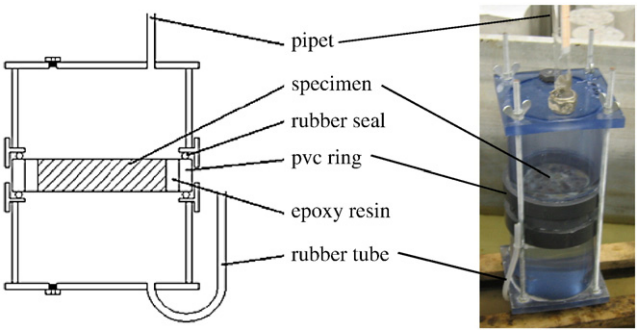

Fig. 3. Water permeability test setup.

T specimen thickness [m]
t time [s]
h_0 and h_f initial and final water heads [cm]

2.4.2. Ultrasonic measurements

The aim of the ultrasonic measurement test was to determine the effect of different crack repair techniques on the propagation of the waves through the concrete specimens. Since ultrasonic waves travel much easier in hardened concrete (4000–5000 m/s) than in water (1480 m/s) or in air (350 m/s), they will travel around an open fissure leading to an increase in transmission time. However, when the crack is sealed, the waves will be able to travel through the sealant and the travel time will be reduced. For each crack repair technique, ultrasonic measurements were carried out in duplicate on concrete prisms of 160 mm × 160 mm × 70 mm with a standardized crack of 0.3 mm width and 10 or 20 mm deep. A Steinkamp ultrasonic tester type BP III with a frequency between 40 and 50 kHz was used for this experiment. This instrument digitizes the time a wave needs to travel from one sensor to the other. Sensors with an exponential shape and a pointed end were used to ensure good contact with the concrete surface and to know exactly the position of the transmitting and receiving points.

Direct transmission measurements were performed at the side surfaces of the specimen parallel to the crack. The sensors were placed, perpendicular to the surface, at 5 locations near the upper end of the specimen, where the crack is located. The obtained values were compared to measurements in the middle and at the bottom end of the specimens, further away from the crack. The different measuring points can be seen in Fig. 4. The transmitting and receiving points were indicated on the specimens, so the same measurements could be

Table 2
Overview of the used crack repair techniques.

A) Traditional							
Type	Description						
Epoxy	Injection of epoxy resin with needle						
Grout	Application of mortar with spatula						
B) Non-traditional							
	Autoclaving bacteria	Injection Levasil	Injection Levasil and BS	Immersion in BS culture	Immersion in $CaCl_2$ and urea solution	Immersion in $Ca(NO_3)_2$ and urea solution	Immersion in $Ca(CH_3COO)_2$ and urea solution
BS + $CaCl_2$				x	x		
Sol–gel		x					
Sol–gel + BS + $CaCl_2$		x		x	x		
BS in sol–gel + $CaCl_2$			x		x		
BS in sol–gel + $Ca(NO_3)_2$			x			x	
BS in sol–gel + $Ca(CH_3COO)_2$			x				x
Autoclaved BS in sol–gel + $CaCl_2$	x		x		x		
Autoclaved BS in sol–gel + $Ca(CH_3COO)_2$	x		x				x

done before and after treatment of the cracks and a comparison could be made of the different repair methods.

2.4.3. Visual evaluation of crack repair

After performing the ultrasonic measurements, a slice of 1 cm was sawn from the samples with standardized cracks, indicated with the dotted line in Fig. 4, in order to obtain cross-sections of the treated cracks. Subsequently the cracks in these slices were viewed under a Moritex Micro Scopeman MS-500B optical microscope which was connected to a camera. The repaired cracks were photographed under magnification and inspected. The same technique was used to examine the repaired cracks at the surface of the specimens used for the water permeability test.

2.4.4. Thermogravimetric analysis

After performance of the water permeability test, specimens treated with (autoclaved) BS in sol–gel + $CaCl_2$ or (autoclaved) BS in sol–gel + $Ca(CH_3COO)_2$ were left to dry through exposure to the air and afterwards a sample of the repair material was removed from the crack by means of a needle. This material was used for thermogravimetric analysis (TGA). For each crack repair technique mentioned above, ±30 mg of the repair material was brought in a sample cup. Subsequently the cup was placed in the apparatus (TA instruments — SDT 2960 Simultaneous DSC-TGA). During the analysis, the crack repair material was exposed to temperatures ranging from 20 °C to 900 °C at a rate of 10 °C/min in an inert argon atmosphere.

Through performance of the TGA analysis, the presence of $CaCO_3$ in the repair material is determined. As the autoclaved bacteria are not expected to precipitate $CaCO_3$ crystals, a difference in weight loss may be seen for treatments with autoclaved or active bacteria. When $CaCO_3$ crystals are present in the repair material, they will decompose into CaO and CO_2 upon heating, according to the reaction below (Eq. (9)).

$$CaCO_3(s) \rightarrow CaO(s) + CO_2(g) \quad (9)$$

As $CaCO_3$ decomposes between the temperature range of 650–750 °C [19] a decrease in weight, caused by the release of CO_2, is expected around that temperature interval for the samples treated with non-autoclaved, active bacteria.

3. Results and discussion

3.1. Water permeability

The water permeability measured was not immediately constant but decreased during several days, as can be seen in Fig. 5. The decrease was supposedly due to incomplete saturation of the specimens and unavoidable existence of air bubbles in the specimens, even though special care had been taken.

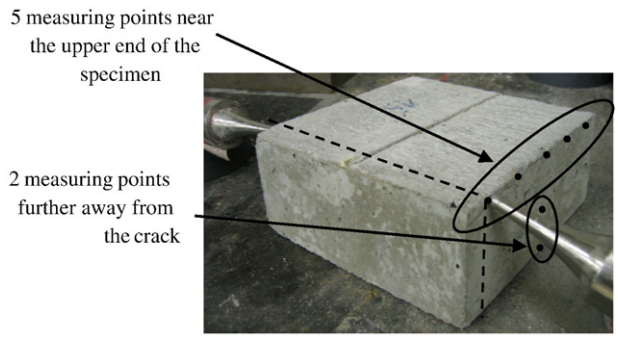

Fig. 4. Ultrasonic transmission measurements with indication of the measuring points (●) and the part of the sample that was sawn off for visual examination (---).

Nanayakkara [20] also observed a decrease in water permeability while performing his tests, but he attributed this to autogenic healing of the cracks. Autogenic healing of cracks in concrete may appear due to further hydration of unhydrated cement particles, carbonation of $Ca(OH)_2$ or dissolution and deposition of soluble hydrates along the flow path. Hearn [21] stated that the decrease in water flow due to continued hydration would have a minimal effect under the condition that specimens were not tested at an early age. The specimens used for this experiment were cured for more than one year in an air-conditioned room with a temperature of 20 °C and a relative humidity above 90%, thus the effect of ongoing hydration could be neglected. Carbonation of $Ca(OH)_2$ can only occur in the presence of CO_2. This phenomenon can also be neglected since specimens were always covered with the water in the upper compartment of the water permeability test setup.

Due to the aforementioned remarks, only air bubbles in the specimen, due to incomplete saturation, could have been responsible for the drop in water flow during the first days. Consequently, measurements were repeated during several days until a steady state flow was reached and all air bubbles were supposed to have disappeared. A steady state flow was considered to be reached when similar results, for the drop in water level, were obtained during 5 subsequent days. The calculated coefficient of water permeability was based on the average of the latest 5 measurements. In Fig. 6, the coefficient of permeability k versus the crack width is shown for the different treatments. In the first graph, results are shown for the traditional repair techniques while in the second graph results for the biological treatments are displayed. In the last graph, a comparison is made of samples treated with active and autoclaved bacteria. To improve the clarity of the graph, water permeability coefficient is shown on a logarithmic scale.

All treatments, except the BS + $CaCl_2$ treatment, resulted in a decrease of permeability when compared to the untreated cracked samples. When the bacteria were not protected against the high pH environment in concrete (BS + $CaCl_2$), no $CaCO_3$ crystals were observed under the microscope, indicating the necessity of using silica gel as filling and protecting agent. Treatment with grout, sol–gel or sol–gel + BS + $CaCl_2$ showed a moderate efficiency. The grains in the grout paste were quite big making it difficult to bring the paste into the crack, which could be a reason for the lower efficiency of this treatment. The treatments with BS in sol–gel + $CaCl_2$ or $Ca(NO_3)_2$ or $Ca(CH_3COO)_2$ resulted in a low water permeability, showing almost an equal performance as epoxy treatments.

Since chloride ions may be harmful to the concrete reinforcement and there is almost no difference in efficiency between BS in sol–gel + $CaCl_2$ or $Ca(NO_3)_2$ or $Ca(CH_3COO)_2$, calcium nitrate and calcium acetate can be used as alternative calcium sources. In their research, De Muynck et al. [13,22] found that the influence of the calcium source is limited to the morphology of the crystals. By means of SEM observations, they proved that the presence of chloride ions resulted

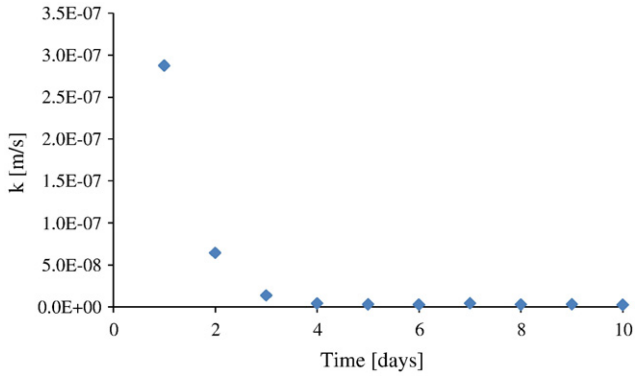

Fig. 5. Decrease in water permeability for a cracked sample treated with sol–gel.

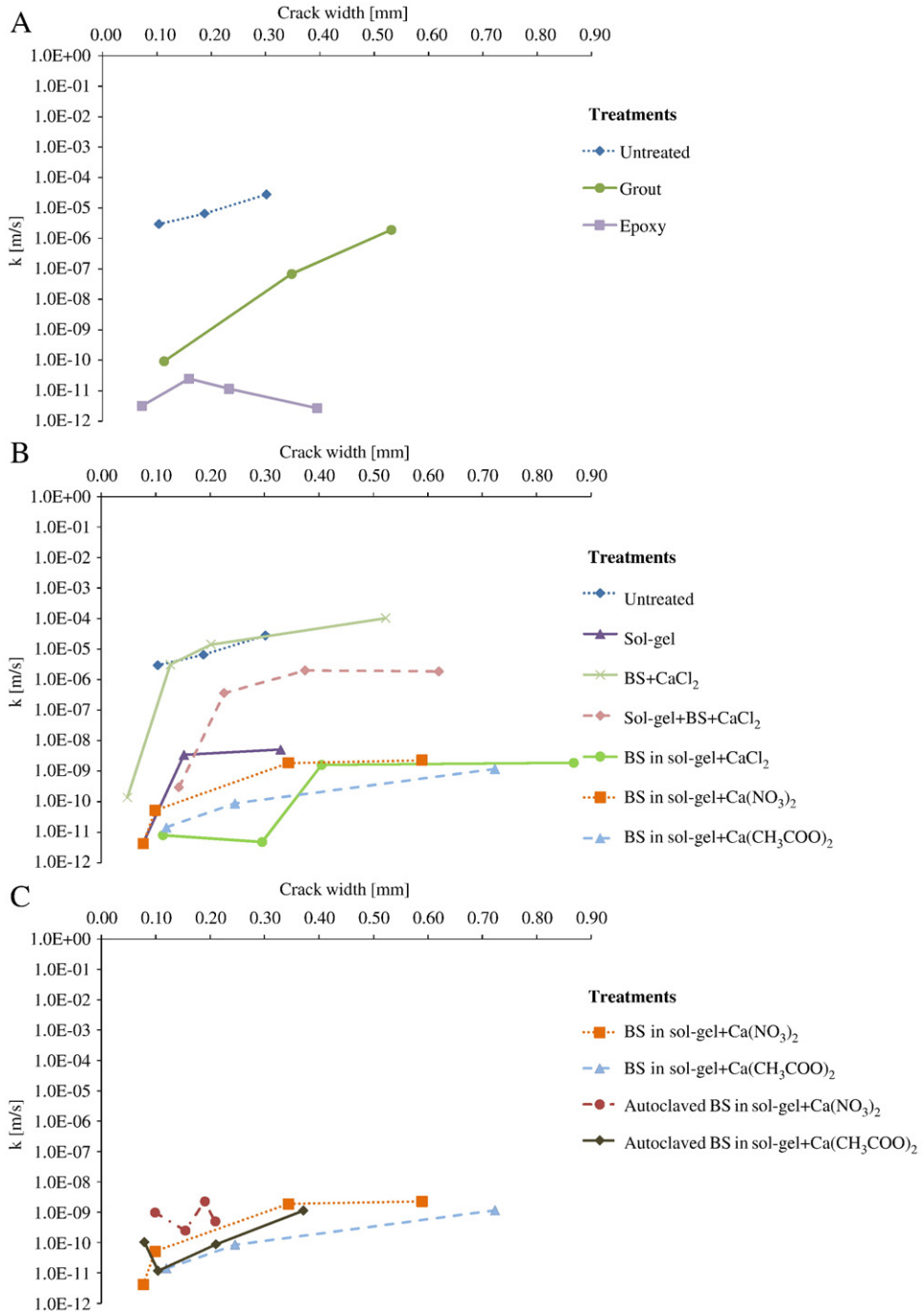

Fig. 6. Water permeability coefficient *k* versus crack width, (A) untreated samples and samples treated with traditional repair techniques, (B) untreated samples and samples treated with biological repair techniques, and (C) comparison of samples treated with living and autoclaved *Bacillus sphaericus*.

in rhombohedral crystals, while the presence of acetate ions resulted in spherical crystals.

In the last graph, a comparison is made between treatments with active and autoclaved bacteria. As it can be seen in the graph, treatment of cracks with autoclaved bacteria in sol–gel also leads to a reasonably large decrease in water permeability. Consequently, the major decrease in water flow may be attributed to crack filling by the silica sol–gel and in the case of treatment with active bacteria a slightly further decrease in permeability may be allocated to the presence of $CaCO_3$ crystals.

As the difference between treatments with active or autoclaved bacteria is not clear from the results of this experiment, TGA analysis was performed on the repair material in the cracks. The results from this analysis are discussed in a subsequent paragraph.

When comparing the coefficient of water permeability *k* obtained in this research for the different treatments with the results obtained by De Belie et al. [1], slightly higher values are observed in this research. This may be due to the fact that crack widths were measured in a different way. However, when comparing the efficiency of the different treatments among each other, the same tendency can be observed in both researches.

3.2. Ultrasonic measurements

Ultrasonic measurements were done before and after treatment of the cracks. Comparing the results, before and after treatment of the cracks, led to the conclusion that transmission time decreased for both

measurements at crack level and measurements further away from the crack. This could be due to further hydration of the concrete specimens. To eliminate the effect of further hydration, the average decrease for the 5 measuring points situated near the crack was corrected with the average decrease for the two other points. This led to different results for the different repair methods. For each crack depth and each repair method, two different samples were treated and examined. The graphs in Fig. 7 show the average relative decrease in transmission time. The standard deviation is indicated by means of error bars.

For the cracks with a depth of 10 mm, treatment with epoxy or BS in sol–gel + $CaCl_2$ gave rise to the highest decrease in transmission time, proving that both techniques are very efficient to heal 10 mm deep cracks. For the other treatments, except the untreated samples and the treatment with sol–gel, a certain decrease in transmission time can also be noticed. Samples treated with sol–gel + BS + $CaCl_2$ and BS + $CaCl_2$ show a bigger decrease than was expected based on the results of the water permeability test and visual evaluation (see further). Here treatments with sol–gel + BS + $CaCl_2$ and BS + $CaCl_2$ seem to perform quite well, but this may be due to the fact that all samples treated with bacteria were placed in a urea–calcium solution for several days which could have led to filling of the submerged pores of the concrete matrix. For the samples treated with sol–gel, only a slight decrease in transmission time could be observed. This could be due to the fact that crack filling with only sol–gel results in shrinkage of the sol–gel. This is also seen from the visual evaluation (see further). Fine fissures in the sol–gel matrix are responsible for the low decrease in transmission time. The untreated samples do not show a decrease but an increase in transmission time. The average decrease at the 2 measuring points further away from the crack was larger than the average decrease for the 5 points situated near the cracks, thus leading to a negative result. This could be due to the fact that there was more hydration in the core of the specimen than at the surface.

For the cracks with a depth of 20 mm, best results were obtained with the epoxy treatment. The BS in sol–gel + $CaCl_2$ or $Ca(NO_3)_2$ or Ca $(CH_3COO)_2$ treatments showed a slightly lower efficiency compared to the results obtained for the 10 mm deep cracks. This is because the latter treatments are not able to completely fill the cracks with a depth of 20 mm which is actually the case for epoxy treatments. This can also be seen in the cross-sections (see further). Samples treated with sol–gel + BS + $CaCl_2$ and BS + $CaCl_2$ again show a bigger decrease in transmission time than was expected. The reason for this is the same as for the 10 mm deep cracks. Treatments with sol–gel and grout show the lowest decrease in time. In the case of the treatment with grout, only the surface of the sample is covered with the grout paste and no filling of the crack occurred, as can be seen in the cross-sections (see further). Although it could be possible that the wave would travel through the bridge of grout paste, only a small decrease in transmission time was observed here, indicating that the waves still travelled around the crack. For the untreated samples again an increase in transmission time is observed, indicating that the crack is not at all filled.

3.3. Visual evaluation of crack repair

In Fig. 8, some top views of the specimens and some cross-sections of the treated cracks are shown. The top views were taken from realistic cracks after the specimens were subjected to the water permeability test. Cross-sections were obtained by sawing samples with repaired standardized cracks after ultrasonic measurements were done.

Fig. 8A shows a non-treated crack. At both crack faces crystal deposition can be observed, showing that the untreated specimens had undergone a certain extent of autogenous healing during the water permeability test. For the specimens with treated cracks, no crystals were observed after performance of the water permeability test. This can be explained as follows: for the untreated samples, the water flow was so fast that the upper compartment, of the test setup, became completely empty between two successive readings. This brought the concrete surface into contact with the atmosphere and led to carbonation of $Ca(OH)_2$ into $CaCO_3$ crystals.

In Fig. 8B, a crack treated with BS + $CaCl_2$ is shown. No $CaCO_3$ crystals were detected by means of the microscope used, probably, because bacteria were not protected against the high pH in concrete. However, when the bacteria are immobilized in sol–gel, complete filling of the cracks occurs as can be seen in Fig. 8C.

Fig. 8D and E show a cross-section of a standard crack filled with grout and epoxy, respectively. Cement grout only covers the surface of the samples and does not fill the cracks because of the big grain size of the grout. Epoxy treatment, by contrast, resulted in complete filling of cracks of both 10 mm and 20 mm deep.

Treatment with only sol–gel or with sol–gel + BS + $CaCl_2$ resulted in cracking of the gel matrix as can be seen in Fig. 8G and H. When the gel hardens, it shrinks and this gives rise to cracking.

Samples treated with BS in sol–gel + $CaCl_2$ or $Ca(NO_3)_2$ or Ca $(CH_3COO)_2$ were placed in a urea–calcium solution immediately after filling of the cracks with silica gel and bacteria. During immersion, bacteria started to precipitate $CaCO_3$ resulting in a compete filling of the cracks (see Fig. 8C). However, complete filling was only feasible for 10 mm deep cracks (see Fig. 8F). As can be seen in Fig. 8I these treatments were not able to fill 20 mm deep cracks. This was also observed from the ultrasonic measurements. 10 mm deep cracks treated with BS in sol–gel + $CaCl_2$ or $Ca(NO_3)_2$ or $Ca(CH_3COO)_2$ performed almost as good as cracks treated with epoxy, which was no

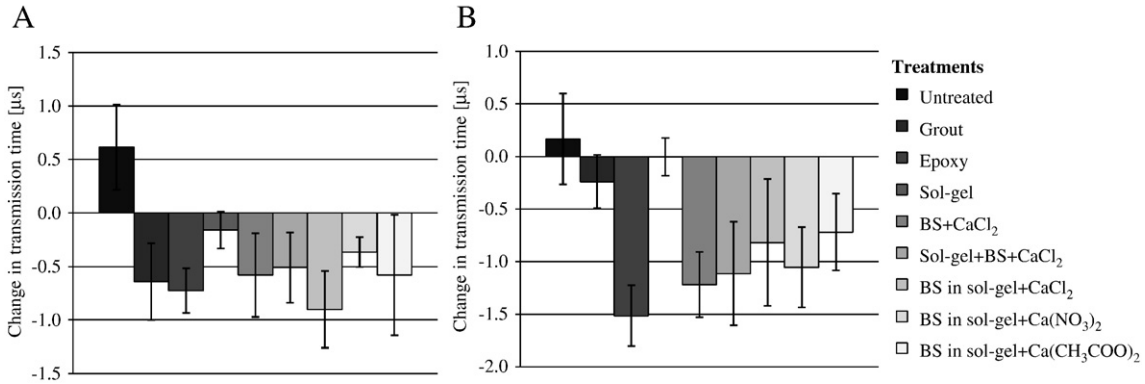

Fig. 7. Relative change in transmission time before and after treatment of the cracks for a crack depth of 10 mm (A) and 20 mm (B). The standard deviation is indicated by means of error bars.

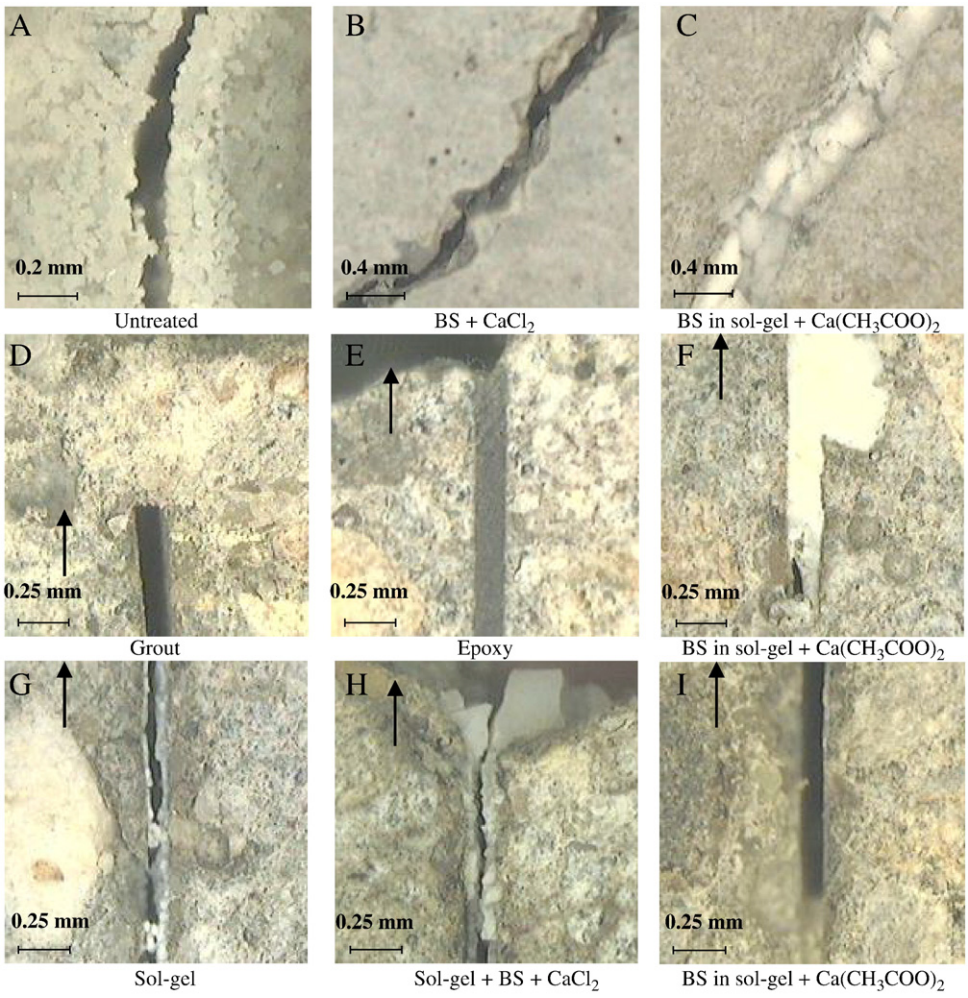

Fig. 8. Top view of an untreated crack (A), crack repaired with BS + $CaCl_2$ (B) or BS in sol–gel + $Ca(CH_3COO)_2$ (C), cross-section of cracks repaired with grout (D), epoxy (E), sol–gel (G), Sol–gel + BS + $CaCl_2$ (H) and cross-section of the tip of a 10 mm (F) and 20 mm (I) deep crack repaired with BS in sol-gel + Ca(CH3COO)2 (upper surface of sample is indicated with an arrow).

longer the case for 20 mm deep cracks, which were only completely filled when epoxy was used.

3.4. Thermogravimetric analysis

Results from the TGA analysis are shown in Fig. 9. In graph A the percentage of weight loss is plotted against the temperature while in graph B the derivative of the weight loss is plotted against the temperature. As it can be seen in Fig. 9A, at about 100 °C the water in the samples, remaining from the water permeability test, evaporates, leading to a decrease in weight. Between 500 and 800 °C another decrease in weight is detected. This may be due to the decomposition of $CaCO_3$. A clear difference in weight loss can be observed between the samples treated with active or autoclaved bacteria. For the autoclaved bacteria the weight loss is rather small (1.69% and 1.34%, for samples with $CaCl_2$ and $Ca(CH_3COO)_2$ as calcium sources, respectively) while for treatment with active bacteria a strong decrease in weight is observed (13.64% and 18.85%, respectively). These results provide evidence that particularly in the case of active bacteria, $CaCO_3$ crystals are formed.

In graph B, the derivative in weight loss is shown versus the temperature to indicate the points at which the weight loss is most apparent. For the repair materials containing autoclaved bacteria, only a small amount of $CaCO_3$ is decomposed at the temperature of 521 °C ($CaCl_2$ as calcium source) and 676 °C ($Ca(CH_3COO)_2$ as calcium source). This decrease in weight may possibly be attributed to chemical precipitation of $CaCO_3$. For the repair materials containing active bacteria, the observed peaks are more distinct and as can be seen in the figure, two different peaks are detected for each material. In the case of treatment with $CaCl_2$ and $Ca(CH_3COO)_2$ as calcium source, the first and second peaks appear at 610 °C and 735 °C and at 628 °C and 768 °C, respectively. Oniyama et al. [19] found that, when $CaCO_3$ was heated at a rate of 10 °C/min, CO_2 was released around 690–760 °C. From these results it can be concluded that the second peak in graph B corresponds with the release of $CaCO_3$ while the first peak corresponds to the evaporation of another material formed by the bacteria. XRD analysis was performed to find out which type of material was formed besides $CaCO_3$. It was shown that the crystalline materials present in the silica gel matrix were calcite, vaterite and aragonite or calcite and vaterite when calcium chloride or calcium acetate was used, respectively. All these are crystalline forms of $CaCO_3$ from which calcite is the most stable form. Aragonite and vaterite undergo transitions to calcite at 455 °C and between 350 and 400 °C, respectively [23]. Consequently above 600 °C the reactant $CaCO_3$ would normally be in the calcite structure and will only correspond to the second peak in the TGA analysis.

From this, it can be concluded that the first peak is caused by the bacteria, because this peak is not present when autoclaved bacteria are used, and that it is not caused by a crystalline material, because it was not detected by means of XRD analysis. Further research has to be done to find out which type of material is formed besides $CaCO_3$.

From the results of the water permeability test, it was seen that both, a combination of sol–gel with active or autoclaved bacteria may

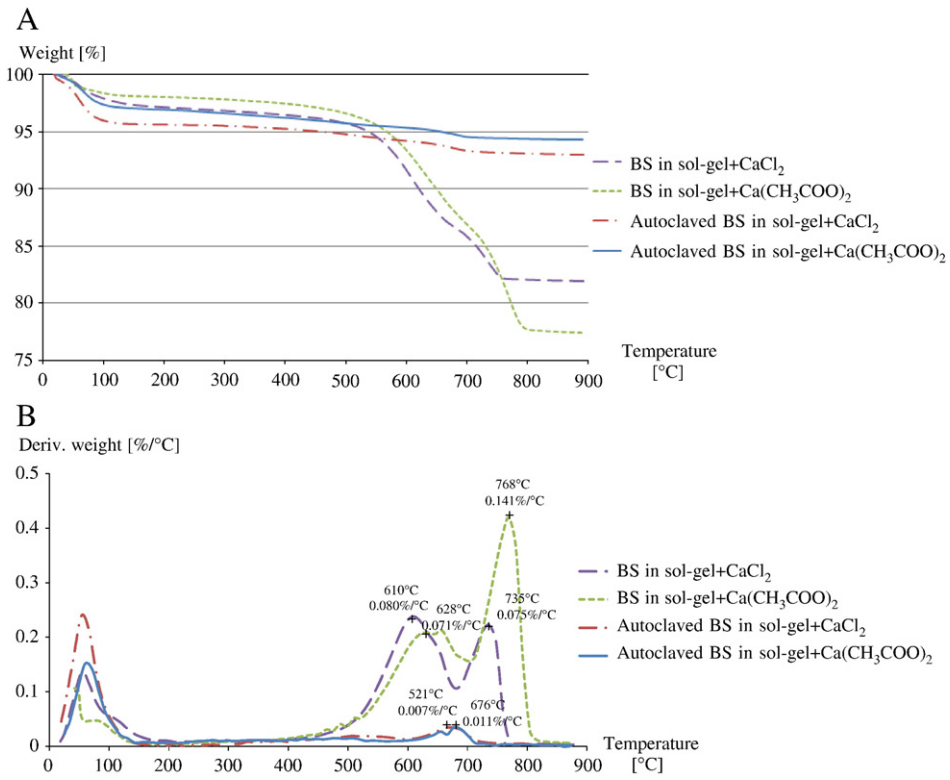

Fig. 9. TGA results for different crack repair materials containing active or autoclaved bacteria, (A) decrease in weight versus temperature, and (B) derivative of weight loss versus increase in temperature.

lead to crack filling and decrease in water permeability. From TGA analysis, however, it is concluded that only active bacteria are able to precipitate $CaCO_3$ crystals in the gel matrix. As it is not sure whether the sol–gel matrix will decompose over time, only the treatment with active bacteria, where crack filling is provided by the gel matrix together with the precipitated $CaCO_3$ crystals, can be seen as a durable repair technique.

4. Conclusions

It appears that some form of enhanced crack repair might be obtained through a biological treatment in which a *B. sphaericus* culture is incorporated in a gel matrix and a calcium source is provided.

In this research, silica gel was used to protect the bacteria against the high pH in concrete. Protection of the bacteria by means of this gel matrix seemed to be effective as $CaCO_3$ crystals were precipitated inside the matrix which was not the case if only bacteria were used, without immobilization in the silica gel.

Crack sealing by means of this biological treatment resulted in a decrease in water permeability. However, it was seen that the decrease in water flow was also obtained if autoclaved bacteria were used instead of active bacteria. This corroborates that the greater part of the decrease in water permeability is attributed to crack filling by the sol–gel matrix. TGA analysis on the crack repair material showed only in the case of active bacteria the presence of $CaCO_3$ crystals. Precipitation of these crystals inside the gel matrix may enhance the durability of this repair material.

Efficiency of this biological treatment was also evaluated by means of ultrasonic transmission measurements and visual examination. Crack treatment with *B. sphaericus*, immobilized in silica gel, resulted in an increase in ultrasonic pulse velocity, indicating that crack bridging was obtained. Visual examination of the cracks proved that this technique resulted in complete filling of the cracks.

The use of this biological repair technique is highly desirable because the mineral precipitation induced as a result of microbial activities is pollution free and natural. However, further experiments have to be done to examine the durability of this crack repair technique.

Acknowledgements

Financial support from the Research Foundation Flanders (FWO-Vlaanderen) for this study (Project No. G.0157.08) is gratefully acknowledged.

Appendix A. Supplementary data

Supplementary data associated with this article can be found, in the online version, at 10.1016/j.cemconres.2009.08.025

References

[1] N. De Belie, W. De Muynck, Crack repair in concrete using biodeposition, International conference on concrete repair, rehabilitation and retrofitting, 24–26 November 2008, Cape Town, South Africa.
[2] U.K. Gollapudi, C.L. Knutson, S.S. Bang, M.R. Islam, A new method for controlling leaching through permeable channels, Chemosphere 30 (1995) 695–705.
[3] S.S. Bang, V. Ramakrishnan, Microbiologically-enhanced crack remediation (MECR), the International Symposium on Industrial Application of Microbial Genomes, Taegu, Korea, 2001.
[4] F. Hammes, W. Verstraete, Key roles of pH and calcium metabolism in microbial carbonate precipitation, Reviews in environmental science and biotechnology 1 (1) (2002) 3–7.
[5] J. Dick, W. Windt, B. Graef, H. Saveyn, P. Meeren, N. De Belie, W. Verstraete, Bio-deposition of a calcium carbonate layer on degraded limestone by *Bacillus* species, Biodegradation 17 (4) (2006) 357–367.
[6] H.M. Jonkers, A. Thijssen, E. Schlangen, Ontwikkeling van zelfherstellend beton met behulp van bacteriën, Cement 4 (2008) 78–81.
[7] H.M. Jonkers, A. Thijssen, O. Copuroglu, E. Schlangen, Application of bacteria as self-healing agent for the development of sustainable concrete, Proceedings of the 1st International Conference on BioGeoCivil Engineering, 23–25 June 2008, Delft, The Netherlands.

[8] K. Santhosh, S.K. Ramachandran, V. Ramakrishnan, S.S. Bang, Remediation of concrete using microorganisms, American Concrete Institute Materials Journal 98 (2001) 3–9.
[9] J.L. Day, V. Ramakrishnan, S.S. Bang, Microbiologically induced sealant for concrete crack remediation, 16th Engineering Mechanics Conference, 16–18 July 2003, Seattle, Washington.
[10] S.S. Bang, J.K. Galinat, V. Ramakrishnan, Calcite precipitation induced by polyurethane-immobilized *Bacillus pasteurii*, Enzyme and Microbial Technology 28 (4) (2001) 404–409.
[11] V. Ramakrishnan, R.K. Panchalan, S.S. Bang, Improvement of concrete durability by bacterial mineral precipitation, Proceedings of 11th International Conference on Fracture, 20–25 March 2005, Turin, Italy.
[12] K.L. Bachmeier, A.E. Williams, J.R. Warmington, S.S. Bang, Urease activity in microbiologically-induced calcite precipitation, Journal of Biotechnology 93 (2) (2002) 171–181.
[13] H. Böttcher, U. Soltmann, M. Mertig, W. Pompe, Biocers: ceramics with incorporated microorganisms for biocatalytic, biosorptive and functional materials development, Journal of Materials Chemistry 14 (2004) 2176–2188.
[14] W. De Muynck, D. Debrouwer, N. De Belie, W. Verstraete, Bacterial carbonate precipitation improves the durability of cementitious materials, Cement and Concrete Research 38 (7) (2008) 1005–1014.
[15] W.S. Rasband, ImageJ, http://rsb.info.nih.gov/ij/ed. Bethesda, Maryland, USA, U.S. National Institutes of Health (1997–2008).
[16] K. Wang, D.C. Jansen, S.P. Shah, A.F. Karr, Permeability study of cracked concrete, Cement and Concrete Research 27 (3) (1997) 381–393.
[17] C.-M. Aldea, M. Ghandehari, S.P. Shah, Member ASCE, A. Karr, Combined effect of cracking and water permeability of concrete (2000).
[18] NBN B 24-213, Belgische norm: Proeven op metselstenen — Wateropslorping onder vacuüm (1976).
[19] E. Oniyama, P.G. Wahlbeck, Application of transpiration theory on TGA data: calcium carbonate and zinc chloride, Thermochimica Acta 250 (1995) 41–53.
[20] A. Nanayakkara, Self-healing of cracks in concrete subjected to water pressure, Symposium on New Technologies for Urban Safety of Mega Cities, 30–31 October 2003, Tokyo, Asia.
[21] N. Hearn, Self-sealing, autogenous healing and continued hydration: what is the difference? Materials and Structures 31 (1998) 563–567.
[22] W. De Muynck, K. Cox, N. De Belie, W. Verstraete, Bacterial carbonate precipitation as an alternative surface treatment for concrete, Construction and Building Materials 22 (5) (2008) 875–885.
[23] A.K. Galwey, M.E. Brown, Thermal decomposition of ionic solids, Studies in Physical and Theoretical Chemistry 86 (1999).